


Combined Soiling and Abrasion Testing of Antisoiling Coatings

Katja Lange, Mohammed A. Bahattab, Saad H. Alqahtani , Mark Mirza, Walther Glaubitt, Volker Naumann , Christian Hagendorf, and Klemens K. Ilse 

Abstract—Soiling of photovoltaic (PV) modules reduces the energy yield and can lead to extremely high losses, especially in desert environments. Therefore, Antisoiling coatings (ASC) are developed to reduce the dust accumulation, but, even if the coating can reduce natural soiling rates, frequent cleaning is still necessary. However, regular cleaning of PV modules by using dry brushes or other technologies can damage the coated glass surfaces. In this article, the damage and abrasion potential of harsh dry brush cleaning is examined for three different ASC, which also possess antireflective (AR) properties. Both changes of antisoiling functionality and antireflective properties are investigated in detail by spectroscopic sample characterization and advanced laboratory soiling tests in a dust chamber. The results indicate significant degradation of the optical and antisoiling properties of the coatings depending on the number of brush cycles used. However, the results suggest that by using more gentle cleaning technologies, the coating functionality could be maintained throughout typical lifetimes of PV modules.

Index Terms—Air pollution, coatings, materials testing, photovoltaic systems, solar energy, solar panels, surface contamination.

I. INTRODUCTION

THE CONTAMINATION of photovoltaic (PV) modules with airborne particles can lead to a significant loss in transmission, decreasing the amount of light that reaches the solar cells [1], [2]. Especially in arid regions, soiling requires frequent cleaning. However, this can have a huge impact on the efficiency of applied solar glass coatings. A promising approach

Manuscript received June 3, 2019; revised August 12, 2019; accepted September 20, 2019. Date of publication November 8, 2019; date of current version December 23, 2019. This work was supported in part by the King Abdulaziz City for Science and Technology. The research and development of the methodology of the abrasion test method was supported in part by the Federal State of Sachsen-Anhalt in the EFRE project “MetroLarge” (IB Sachsen-Anhalt, 1804/00012) and in part by the Federal Ministry of Economic Affairs and Energy of Germany in the project “ROSE” (BMW, 03TNH022A). (Corresponding author: Klemens K. Ilse.)

K. Lange, V. Naumann, C. Hagendorf, and K. K. Ilse are with the Fraunhofer Center for Silicon Photovoltaics CSP, D-06120 Halle (Saale), Germany, and also with the Fraunhofer Institute for Microstructure of Materials and Systems IMWS, 06120 Halle (Saale), Germany (e-mail: katja.lange@csp.fraunhofer.de; volker.naumann@csp.fraunhofer.de; christian.hagendorf@csp.fraunhofer.de; klemens.ilse@csp.fraunhofer.de).

M. A. Bahattab and S. H. Alqahtani are with the King Abdulaziz City for Science and Technology KACST, Riyadh 12354, Saudi Arabia (e-mail: bahattab@kacst.edu.sa; shalqahtani@kacst.edu.sa).

M. Mirza and W. Glaubitt are with the Fraunhofer Institute for Silicate Research ISC, D-97082 Würzburg, Germany (e-mail: mark.mirza@isc.fraunhofer.de; walther.glaubitt@isc.fraunhofer.de).

Color versions of one or more of the figures in this article are available online at <http://ieeexplore.ieee.org>.

Digital Object Identifier 10.1109/JPHOTOV.2019.2945192

to reduce the problem of soiling is the application of antisoiling coatings (ASC). These coatings are supposed to decrease the amount of dust that sticks to the glass surface, while also possessing antireflective (AR) properties, as has been shown in previous studies [3], [4]. In order to achieve the AR effect of glass coatings, a certain porosity of the coatings may be required, which can make them sensitive to mechanical abrasion. The abrasion could change the coating properties significantly, potentially leading to a reduction or loss of AR and AS properties if the coatings are completely removed.

Within this article, three different ASC developed by Fraunhofer ISC and KACST are tested for their effectiveness and resistance against cleaning abrasion. For this purpose, different numbers of cleaning cycles were simulated using a dry brush test developed at Fraunhofer CSP. Along with the transmission loss after abrasion, the antisoiling functionality of the stressed samples was investigated by artificial dust deposition in a dust chamber and by a rotational force test method developed at Fraunhofer CSP and Anhalt University [5], [6]. All test procedures used are based on industry standards, some of which have had to be adapted to meet PV application and cleaning scenarios.

II. EXPERIMENTAL

A. Samples

Three different antisoiling coatings (with antireflective properties) and an uncoated reference glass were investigated in this article. The coatings were applied to both sides of 10x10 cm² solar grade float glass by sol–gel technology and mainly consist of nanoporous SiO₂ and exhibit different morphologies and surface properties. Coating 1 contains nanoparticles with a broad particle size distribution, whereas Coating 2 is composed of a combination of silica nanoparticles of two size ranges (<10 nm and >60 nm) and Coating 3 possesses a comparably narrow size distribution. Exemplary scanning electron microscopy images of similar coating structures are shown in [3], [4]. All coatings are hydrophilic.

Sample batches of one uncoated reference glass and three differently coated glasses were used for the experiments, whereby overall four sample batches were exposed to a different number of cleaning cycles and successive soiling tests, see Fig. 1. Apart from the number of abrasion cycles, the tests were performed on all samples with the same parameters during soiling, light microscopy, rotational force test, and transmittance measurements. Gloves were worn, while working with the specimens to prevent

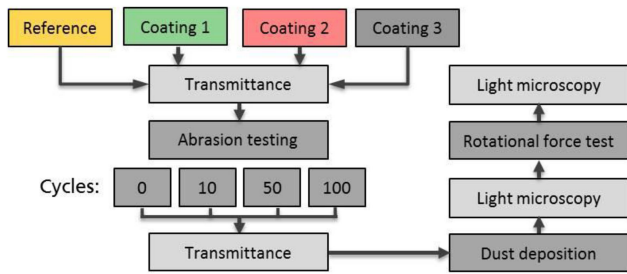


Fig. 1. Schematic overview of the experimental procedure of performed abrasion and soiling tests for three ASC and an uncoated reference glass.

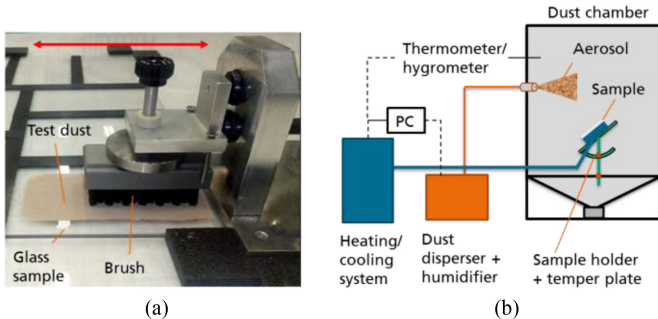


Fig. 2. (a) Abrasion test setup with brush and test dust on top of the glass sample. (b) Schematic representation of dust chamber used for laboratory soiling tests.

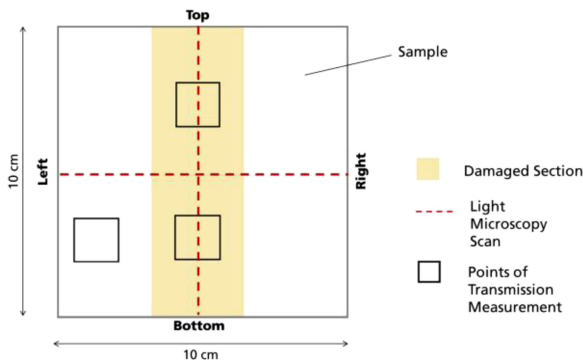


Fig. 3. Position of abrasion, transmission measurements, and light microscopy line scans on the square glass samples.

damage or changes to the coatings because of contact with the skin or other contamination.

B. Abrasion/Cleaning Testing

In order to simulate the process of cleaning with a dry brush, an abrasion tester was developed at Fraunhofer CSP. The method consists of a forward and backward moving arm to which a brush is attached, moving over the dusted test samples (see Fig. 2) with an average speed of approximately 24 cm/s (according to ISO 11998 and DIN EN 1096-2 Appendix E). The brush was selected according to the ASTM D2486 standard, having a total weight of 454 g and 19 mm long bristles made of nylon arranged in a 5/4 pattern. The brush dimensions are not wide enough to cover the entire square sample area, so only one strip in the center of the samples is damaged during testing (see Fig. 3). The advantage of this is that, after abrasion, transmittance measurements can

also be carried out on the undamaged areas in order to assure a better comparison with the stressed coating.

The abrasion tests were carried out at dry conditions, whereby 1 g of Arizona Test Dust A2 fine (ISO 12103) was homogeneously spread over the sample surface in the beginning of each experiment, corresponding to an extremely high dust load. The brush was then placed on top of the dust layer and moved back and forward for a certain number of cycles, see Fig. 2(a). It should be noted that the short, comparably stiff bristles of the brush are perpendicular to the specimen surface and do not bend during the abrasion process. Together with the abrasive dust, this test procedure is intended to simulate a worst-case scenario for dry cleaning of PV modules.

For each sample batch, 0, 10, 50, and 100 abrasion cycles were performed, with one cycle consisting of one back and forth movement of the brush. Assuming one cycle to reflect one manual cleaning operation in the field, 100 cycles could correspond to 25 years of field operation cleaning every three months.

C. Laboratory Soiling Test

The used soiling test setup consists of a dust chamber in which the samples can be placed at defined tilt (here: 20°), see Fig. 2(b) as well as [5], [6]. The relative humidity and temperature of air and sample surfaces can be regulated within the chamber. One batch of four samples (10 × 10 cm) can be tested at the same time. The loaded samples had 15 min to adapt to the environmental parameters ($55.4 \pm 0.4\%$ RH, 20.6 ± 0.2 °C sample temperature and 22.7 ± 0.2 °C air temperature) before the aerosol of Arizona Test Dust A2 fine was introduced into the chamber for about 1 min. After that, the samples remained in the test chamber for a further 30 min to allow the dust to settle mainly via sedimentation (gravitational settling), homogeneously covering the sample surfaces. It was ensured that all soiling procedures took place on the same day, as otherwise the parameters of the ambient air in the laboratory and outdoors (temperature, relative humidity) could vary, leading to potential deviations in the results.

Subsequently to the process of dust deposition, all samples undergo sample characterization by light microscopy to check for homogeneity of dust deposition and potential influence of the particle *rebound* during deposition, which is characterized by particles bouncing off the surface during impact [5]–[7].

This is followed by dust removal experiments. In desert regions primarily wind is considered to contribute to self-cleaning of the coatings between the rare rain events. Therefore, it was investigated to which extend the deposited dust can be removed at dry conditions. For a reproducible simulation of a huge range of wind cleaning forces acting in parallel to the sample surface in only one experiment, centrifugal forces were applied to the dust particles. For the so-called rotational force test [5], [6], the samples were placed horizontally into a spin coater by *Laurell Technologies* and rotated at 3000 rpm for about one minute. In this manner, the dust particles can be removed in a controlled way using defined centrifugal forces, and the process of removal is called *resuspension* in the following, see also [7].

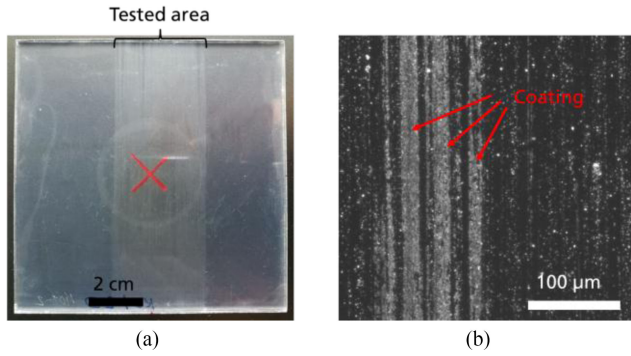


Fig. 4. (a) Photograph of a coated glass sample after 50 cycles of abrasion. The red marking denotes the sample center around which the sample was rotated during rotational force test. (b) Light microscopy image of position close to sample center.

D. Sample Characterization

In order to investigate the antireflective properties, hemispherical transmittance measurements were performed on all samples before and after abrasion, using the spectrophotometer *Perkin Elmer LAMBDA 1050* with an 150 mm integrating sphere. Each sample was examined at different positions (see Fig. 3). Two measurements were carried out in the abrasion area in order to account for potential inhomogeneities of the coating abrasion. In addition, one measurement was performed in the undamaged area so that potential changes of the coatings because of processing and sample handling could be examined. The transmittance of light was measured in the wavelength range of 400–1200 nm.

To determine the surface coverage (percentage of sample area covered by dust) of the dusted glass samples after dust deposition and removal experiments, the samples were examined using the *Carl Zeiss Axio A1* light microscope. Dark-field illumination was applied because it creates a particularly high optical contrast between the glass surface and the dust particles on it. Here, a large number of images was taken of each sample performing line-scans, with the images extending over the entire width of the glass samples (see dotted lines in Fig. 3). Accordingly, deviations between the edge and center of the glass can be characterized, which is necessary for the evaluation of rotational forces tests. The images were examined using the software *ImageJ* and the default auto-threshold function (varied IsoData algorithm)¹ which determines the percentual surface coverage of each sample.

III. RESULTS AND DISCUSSION

A. Visual and Microscopy Inspection After Abrasion Testing

The visual and microscopy inspection after abrasion testing in Fig. 4 show a glass sample with Coating 2 after 100 cycles of abrasion. The picture on the left shows a photograph of the damaged sample, and on the right one some visible scratches in the dark field light microscopy. The damaged area is clearly visible in photography, and the bright scratches in the microscopic image indicate that parts of the coating are damaged

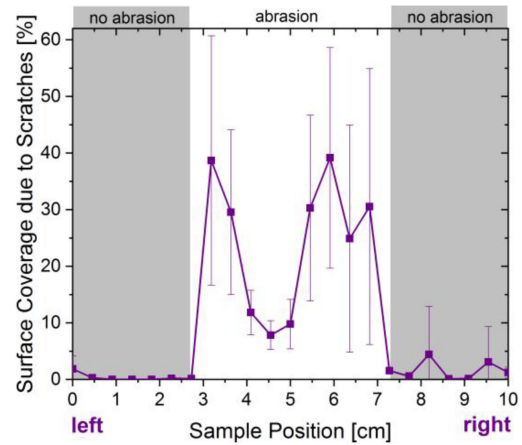


Fig. 5. Surface coverage because of scratches on glass sample with Coating 2 after 100 cycles of abrasion, before dusting. Grey: Area without abrasion, white: Area with abrasion.

or—in parts—completely abraded, which will be investigated by transmittance measurements in the next section.

The scratches caused by the abrasion which are visible in light were also evaluated by image analysis as demonstrated in Fig. 5, applying the same *ImageJ* methodology as used for particle detection. The surface coverage caused by scratches is shown over the entire sample width, showing areas with and without abrasion. The sample shown in Fig. 5 is Coating 2 after 100 cycles of abrasion (without dusting). The areas in which no abrasion was performed are highlighted in grey. Here, the surface coverage caused by scratches is close to zero. Slight deviations are because of impurities on the glass surface. In the area of abrasion, the surface coverage immediately increases significantly because the damaged surface is no longer smooth but shows scratches. The light-microscopy analysis indicates that the abrasion is not homogenous for the complete abraded area, as the surface coverage decreases slightly toward the sample center. This is potentially attributed to the fact that the coating is so badly damaged that it is mostly removed. Accordingly, the mostly intact, uncoated glass surface appears black in the microscopic dark field [see Fig. 4(b)] and is much less prone to abrasion as it shows no visible scratches.

B. Hemispherical Transmittance and Transmission Loss

Transmittance measurements were performed for each sample prior and after abrasion tests. The diagrams in Fig. 6 show exemplary transmittance results of undamaged samples (0 cycles) and after 100 cycles of abrasion testing.

It should be noted that the glass samples were processed by dip coating, leading to coatings on both front and backside. In order to account for the AR effects of the backside, which are not relevant to this article, the equivalent transmittance for a single side coating T_{single} (where only one side of the specimen was abraded) was determined theoretically from the measurement data T_{meas} by the simple approximation

$$T_{\text{single}} \approx T_{\text{meas}} - (T_{\text{double}} - T_{\text{ref}}) / 2 \quad (1)$$

¹[Online]. Available: https://imagej.net/Auto_Threshold

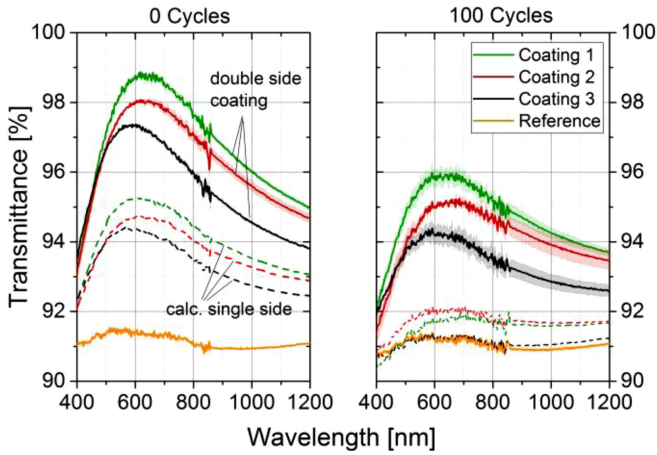


Fig. 6. Transmittance of glass with three different ASC (with antireflective effect) and one uncoated reference glass after 0 and 100 cycles of abrasion with dry brush. The dotted line denotes calculated transmittance for single side coatings.

with T_{ref} being the transmittance of the uncoated reference glass and T_{double} being the initial transmittance measured after 0 cycles. The calculated spectra T_{single} are given by the dotted lines in Fig. 6.

The undamaged coatings (0 cycles in Fig. 6) exhibit clear antireflective properties compared with uncoated solar glass with increased transmittance of at least 6% (3% for single side coating) in the wavelength range between 500 and 700 nm. This also results in a clear coating ranking with respect to antireflective properties: Coating 1 > Coating 2 > Coating 3.

Furthermore, it is clearly demonstrated that the transmission drops after 100 cycles of abrasion for the coated samples compared with the uncoated reference, which remains at the same level. Accordingly, the test procedure does not alter the hemispherical transmittance of bare solar glass, which can be attributed to the fact that there are much less or no scratches in the glass (see previous section), and scratches also do not lead to significant changes as they only increase the fraction of scattered light but not the overall hemispherical transmittance, see also [8].

From the measurement results of the double-side coated glasses after abrasion testing, the coating ranking seems to remain constant. However, this ranking is attributed to antireflective effects of the coated glass backside, which remains undamaged. In contrast, from the calculations of T_{single} , it can be concluded that after 100 brush cycles, Coating 3 completely lost its antireflective properties, whereas Coating 2 and Coating 1 still exhibit an AR effect, and Coating 2 now outperforms Coating 1. This is also an important notice for intercomparison of abrasion behavior of various coatings which are deposited on two or only one sample side.

Fig. 7 shows the results of integral transmission loss for the different numbers of brush cycles and different coatings, normalized to the initial coating performance. The integral transmission loss T_{Loss} was calculated as follows:

$$T_{\text{Loss}} = \frac{\sum_{\lambda=400 \text{ nm}}^{1200 \text{ nm}} (T_{\text{single,abr}}(\lambda) - T_{\text{single,ini}}(\lambda))}{\sum_{\lambda=400 \text{ nm}}^{1200 \text{ nm}} T_{\text{single,ini}}(\lambda)} \quad (2)$$

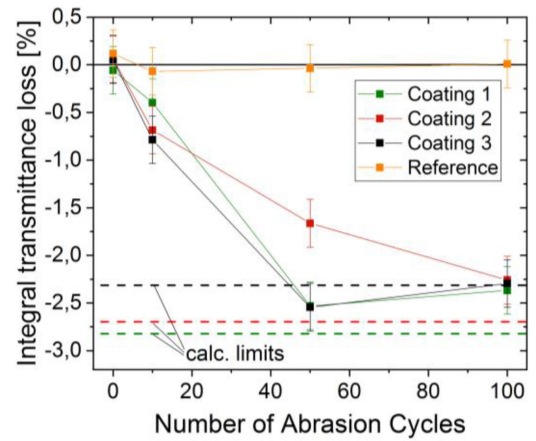


Fig. 7. Integral transmittance loss of solar glass with three different ASC and one uncoated reference glass for different numbers of cleaning cycles with a dry brush. The dotted lines indicate the maximum possible transmittance loss for the case that the complete coatings are removed.

with $T_{\text{single,ini}}$ and $T_{\text{single,abr}}$ being the transmittance calculated after (1) for the samples before and after abrasion, respectively. The transmittance loss can be assumed to directly correlate with the power output losses of PV modules [1], [9].

While the transmission loss of the uncoated sample persists nearly constant in Fig. 7 ($\sim 0\%$), the coated samples show decreasing values with increasing brush cycles. Coating 1 and 3 exhibit similar behavior: After ten cycles of abrasion they lose approximately 0.5–0.75% of their transmittance, after 50 cycles the values settle at -2.5% and do not decrease, even after 100 cycles. However, although Coating 1 and 3 show a similar decrease in optical performance, the difference is the calculated limit (dotted lines) at which the coating should be completely removed. Fig. 7 indicates that the antireflection effect of Coating 3 was completely removed already after 50 cycles with only minor deviations in the near infrared. Fig. 7 shows the same effect and suggests that, even with greater numbers of abrasion cycles, these values do not decrease further, which again indicates that brushing the (now uncoated) glass does not lead to significant optical losses. In contrast, in the case of full coating abrasion, the AR performance of Coating 1 should have led to transmission losses of almost -3% , but this value has not yet been achieved, even after 100 abrasion cycles. Accordingly, Coating 1 can be regarded to be more abrasion resistant than coating 3.

Regarding Coating 2, a higher stability is indicated for 50 abrasion cycles (-1.5% compared with -2.5% for Coating 1 and 3), although the absolute transmission losses are very similar to the other coatings after 10 cycles (-0.75%) and after 100 cycles (-2.25%). The limit to the completely removed coating has not yet been reached, which is approximately -2.62% . This indicates that, even after strong abrasion with 100 brush cycles, a residual antireflective coating is still present on the specimen.

In summary, the abrasion and its relevance for the AR performance of coatings can change quite significantly with the number of applied cleaning cycles. From the presented results, Coating 1 initially possesses the highest transmittance values, but is not as stable as Coating 2.

Regarding the stability of the test and characterization methods, different potentially influencing factors have been identified. Deviations like the ones observed for Coating 3, exceeding the estimated AR limits after 50 cycles, can be attributed to the measurement uncertainty of the transmission measuring instrument (i.e., $\pm 0.2\%$), and to the problem that varying humidity can lead to fluctuations in the antireflection effect especially in porous layers. This is due to the fact that at higher relative humidity, water could adsorb in the pores due to capillary condensation, and thus, the refractive index of the coating is changed. In addition, potential influences of remaining dust contamination or other altering effects of the remaining but stressed coatings could influence the transmittance results.

As stated in the experimental section, the used artificial abrasion test is intended to simulate a worst-case scenario for dry cleaning of PV modules. In contrast, in industry applications, softer and rotating brushes are typically used to clean the PV modules, reducing the mechanical stresses on the coatings. For instance, some first field studies as reported in [8], [10] indicated numerous scratch patterns on various coated glass coupons for dry brush cleaning after one year of monthly cleaning, but less damages for wet-sponge squeegee cleaning.

However, the comparison between realistic degradation of coatings in the field and artificial abrasion tests is still subject to research. This is mainly due to the various existing cleaning methods (manual and automated), various coating types, and other factors like locally dependent soiling rates, dust properties, and cleaning frequency. Furthermore, it should be noted that test results from small laboratory samples do not necessarily represent the performance of industrial applied coatings, as process parameters (e.g., during roller coating and glass tempering) could change coating properties. In addition, numerous different laboratory abrasion test methods have been proposed [11], which is also reflected in actual standardization efforts.²

C. Soiling Test Results

Subsequent to the abrasion testing, soiling tests were performed to investigate the persistence of the antisoiling functionality under dry conditions. As a first step, the four samples of one sample batch (i.e., according to the number of abrasion cycles) were exposed to a controlled dust atmosphere in a dust chamber [see Fig. 2(b)] at the same time. The method of dust deposition by gravitational settling is typically very homogenous over the full sample areas if uncoated glasses are used, as has been shown in [5].

After dust deposition, the samples were scanned under the light microscope once from top to bottom and once from left to right (see Fig. 3) over the full sample width. It should be noted that the scan from top to bottom is done completely in the damaged area and the scan from left to right includes undamaged surface at the edges as well as the damaged areas toward the center of the samples. From the light microscopy images, the surface coverage was determined with respect to sample position using *ImageJ*.

²IEC 62788-7-3 ED1 Measurement procedures for materials used in photovoltaic modules - Part 7-3: Environmental exposures—Accelerated abrasion tests of PV module external surfaces.

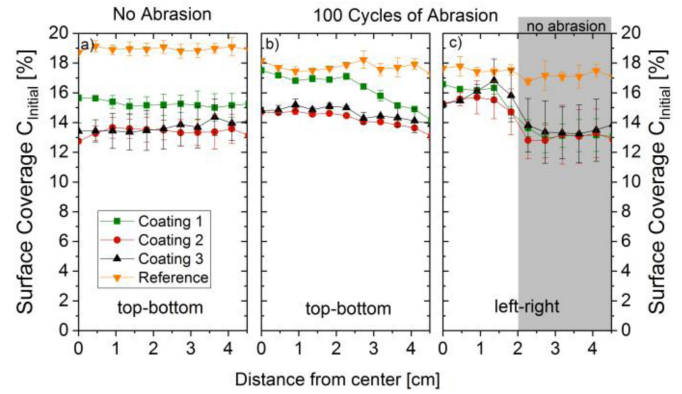


Fig. 8. Surface coverage for three different antisoiling coatings and one uncoated reference glass after 0 (a) and 100 cycles (b, c) of abrasion after dusting but before sample rotation, depending on the distance from sample center.

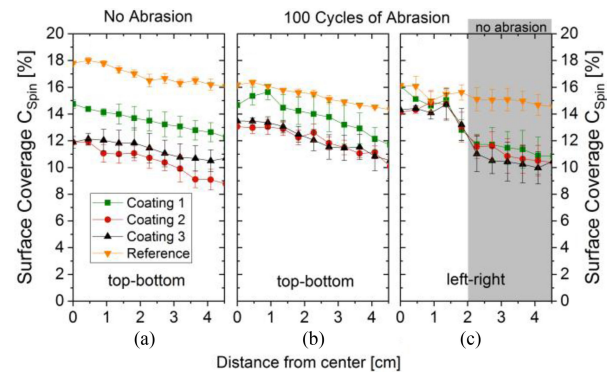


Fig. 9. Surface coverage for three different antisoiling coatings and one uncoated reference glass after 0 (a) and 100 cycles (b, c) of abrasion after dusting and subsequent sample rotation, depending on the distance from sample center. The particle-removing centrifugal force increases with distance from sample center, see further details in [5].

Exemplary data of surface coverage after dust deposition is shown in Fig. 8: For samples with no abrasion Fig. 8(a) and for the samples after 100 cycles of abrasion including both line-scans from top to bottom Fig. 8(b), and left to right Fig. 8(c). The data is represented depending on the distance from the sample center. For the individual samples without abrasion, the surface coverage is relatively homogeneous for the whole sample surfaces. However, the coated samples indicate a remarkably lower surface coverage compared to the uncoated reference glass with reductions of 20–30%. These results are possibly attributed to the effect of rebound: for low-adhesive surfaces such as Coatings 1–3, the required kinetic energy of particles for bouncing off the surface during impact will be less compared with uncoated surfaces.

Accordingly, more particles can bounce off the surface during dust deposition, even for particle settling velocities occurring during gravitational settling, as has been shown in [6]. The lower adhesion forces for the coatings used in this article are possibly attributed to lower Van-der Waals interactions because of an increased surface roughness in the nm-range.

After the abrasion experiments, the lateral homogeneity of surface coverage changes significantly [see Fig. 8(b) and (c)],

which we attribute to inhomogeneous surface abrasion. In addition, the observed benefits from rebound effects decrease significantly in the regions of abrasion, as is vividly demonstrated by Fig. 8(c) for areas with and without abrasion. However, there are some differences observed for the different coatings, and from Fig. 8(b) it can be concluded that rebound effects can be still beneficial after 100 cycles of abrasion. The coating ranking will be discussed in more detail based on a comparison of the test results from all performed soiling experiments (see Fig. 10).

After dust deposition, the samples were rotated at 3000 rpm reinvestigated by light microscopy in order to evaluate the dust removal efficiency at controlled removal forces. Fig. 9 shows exemplary results that after the rotational force test for the same samples as in the previous section, depending on the distance from sample center. In direct comparison for the individual samples in Fig. 8 and 9, it can be seen that the surface coverage is lower after the dust removal experiment for all sample types. In addition, there is a decrease of surface coverage toward the edge of the sample, because of the centrifugal forces during the spin increase with increasing distance from the sample center. Similar to the results after dust deposition, all coated surfaces possess a significantly reduced surface coverage after dust removal compared with the uncoated reference, especially for the nonabraded samples. This increased particle resuspension can also be attributed to reduced adhesion forces between the particles and the coated sample surfaces. However, the difference in surface coverage between uncoated and coated samples decreases significantly after 100 abrasion cycles, which clearly indicates a reduced antisoiling functionality because of abrasion.

In order to better compare the data from the different coatings and abrasion cycles, average values of the surface coverage in the areas with abrasion were calculated for each sample, both before and after rotational force tests. In addition, to account for possible influences of possibly changing parameters during the dust deposition processes of the different samples batches, the surface coverage of each coated sample C_{coating} was normalized the results of the reference sample C_{Ref} of the same sample batch, i.e., which has undergone the same number of abrasion cycles and test conditions. Accordingly, the relative surface coverage C_{rel} was defined as

$$C_{\text{rel}} = C_{\text{coating}} / C_{\text{Ref}} \quad (3)$$

and calculated both for the results directly after dust deposition and after rotational force test in order to account for the effects of both rebound and resuspension.

The results of all soiling experiments are shown in Fig. 10, enabling a comparison of coating ranking and performance change with increasing abrasion cycles. Initially, for the case of no abrasion, Coating 2 demonstrates the lowest relative surface coverage both for rebound (before spin) and resuspended (after spin) particle fractions, followed by Coating 3 and Coating 1. Accordingly, it is expected that Coating 2 also permits the best antisoiling functionality at dry environmental conditions. With the exception of a few values, this ranking remains stable for different numbers of cleaning cycles. However, the indicated standard deviation makes the interpretation more difficult. The deviations of coating ranking might be attributed to changes in

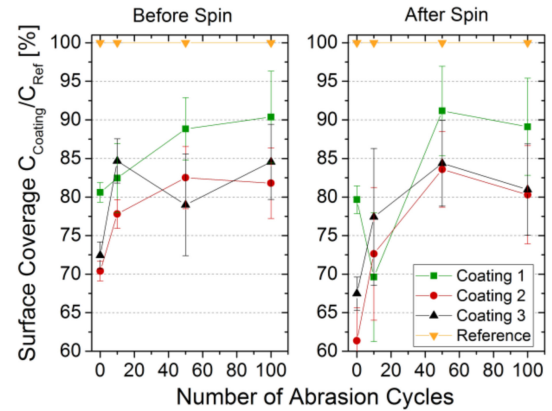


Fig. 10. Relative surface coverage results from performed soiling test for three different ASC in comparison to uncoated glass (100%) before and after the rotational force test.

inhomogeneous surface coating abrasion, e.g., causing different physical surface properties as well as background noise during light microscopy. In addition, an analysis with respect to particle sizes could increase the accuracy and reduce the deviations in accuracy because of the strong particle size dependency of particle adhesion and removal forces [2], [6], but was out of the scope of this article.

Irrespective of the coating ranking, there is a clear trend that the surface coverage increases with the number of abrasion cycles for all coatings, both after deposition and after rotational force test. This indicates that with increasing damage to the coating as already indicated from optical performance, also the antisoiling functionalities of increased rebound and resuspension are impaired and the coatings become less effective. It is assumed that this degradation is mainly attributed to a mechanical deterioration of the coating morphologies and to a less extent to surface contamination. Nevertheless, the uncoated reference sample always shows the highest values of surface coverage. This means that, even damaged coatings after very heavy abrasion (100 brush cycles) without antireflective properties could still possess an antisoiling functionality and work better than none at all. A potential explanation for this behavior is that a thin layer of nanoparticles, of which the coatings are composed, may not be removed during abrasion tests, but still creates favorable surface properties for antisoiling effects (e.g., surface roughness in the nm-scale). In contrast, for antireflective properties, the nano-porous coating needs a certain coating thickness.

IV. CONCLUSION

Combined abrasion and soiling tests were performed using three different ASC and uncoated reference glasses. For abrasion testing, dry, linear brushing with Arizona test dust (A2) between the brush and the surfaces was used, simulating a worst-case application scenario of harsh manual cleaning. For soiling tests, Arizona test dust was deposited in a chamber by sedimentation from an aerosol at dry environmental conditions and the dust removal efficiency was determined using a rotational force test.

It was shown that the undamaged coatings possess superior antireflective properties with an increase in light transmittance

of more than 3% at about 600 nm. In addition, all coatings indicate notably increases of 20–30% of particles rebounding from the surface during dust deposition, as well as an increased resuspension after the rotational force tests. Coating 1 indicated the best AR-effect, but the lowest AS functionality, and Coating 2 indicates the best antisoiling effects. However, the investigated glass coatings show a decrease of both antireflective and antisoiling properties with increasing number of brush cycles, whereas the uncoated glass indicates no significant changes. Even after 100 brush cycles, Coating 1 and 2 still indicate positive AR effects and all coatings still show an antisoiling functionality.

Lateral inhomogeneities due the abrasion test procedure are considered the major uncertainty factor within this article, as they may lead to differences in surface and coating properties which could affect both the optical performance as well laboratory soiling testing. More research and improved methods are needed here to assure a homogenous abrasion also for large sample areas.

The simulated abrasion test and results obtained for 100 cycles is likely equivalent to the damage after harsh and dry manual cleaning every three months for 25 years. Even for such a harsh scenario, especially Coating 2 can still possess AR- and AS functionalities. Since it is assumed that the damage potential is significantly reduced by using softer rotating brushes and water (typical for commercial cleaning machines), the coating properties could possibly be maintained over the typical lifetime of PV modules if such optimized cleaning techniques are used. However, more work is needed in order to better correlate the artificial soiling behavior to real soiling and the accelerated abrasion to actual abrasion in the field.

REFERENCES

- [1] T. Sarver, A. Al-Qaraghuli, and L. L. Kazmerski, “A comprehensive review of the impact of dust on the use of solar energy: History, investigations, results, literature, and mitigation approaches,” *Renew. Sustain. Energy Rev.*, vol. 22, pp. 698–733, 2013.
- [2] K. K. Ilse *et al.*, “Fundamentals of soiling processes on photovoltaic modules,” *Renewable Sustain. Energy Reviews*, vol. 98, pp. 239–254, 2018.
- [3] M. A. Bahattab *et al.*, “Anti-soiling surfaces for PV applications prepared by sol-gel processing: Comparison of laboratory testing and outdoor exposure,” *Sol. Energy Mater. Sol. Cells*, vol. 157, pp. 422–428, 2016.
- [4] W. Glaubitt and P. Löbmann, “Anti-soiling effect of porous SiO₂ coatings prepared by sol-gel processing,” *J Sol-Gel Sci Technol*, vol. 59, no. 2, pp. 239–244, 2011.
- [5] K. K. Ilse *et al.*, “Advanced performance testing of anti-soiling coatings: Part I: laboratory test setup and experimental results,” *Sol. Energy Mater. Sol. Cells*, to be published, 2019, doi: [10.1016/j.solmat.2019.110048](https://doi.org/10.1016/j.solmat.2019.110048).
- [6] K. K. Ilse *et al.*, “Advanced performance testing of anti-soiling coatings: Part II: particle-size dependent analysis and determination of adhesion forces,” *Sol. Energy Mater. Sol. Cells*, to be published, 2019, doi: [10.1016/j.solmat.2019.110049](https://doi.org/10.1016/j.solmat.2019.110049).
- [7] B. Figgis, A. Ennaoui, S. Ahzi, and Y. Rémond, “Review of PV soiling particle mechanics in desert environments,” *Renew. Sustain. Energy Rev.*, vol. 76, pp. 872–881, 2017.
- [8] S. Toth *et al.*, “Soiling and cleaning: Initial observations from 5-year photovoltaic glass coating durability study,” *Solar Energy Materials Solar Cells*, vol. 185, pp. 375–384, 2018.
- [9] K. K. Ilse *et al.*, “Comprehensive analysis of soiling and cementation processes on PV modules in Qatar,” *Solar Energy Materials Solar Cells*, vol. 186, pp. 309–323, 2018, doi: [10.1016/j.solmat.2018.06.051](https://doi.org/10.1016/j.solmat.2018.06.051).
- [10] A. Einhorn *et al.*, “Evaluation of soiling and potential mitigation approaches on photovoltaic glass,” *IEEE J. Photovolt.*, vol. 9, no. 1, pp. 233–239, Jan. 2019.
- [11] D. C. Miller, M. T. Muller, and L. J. Simpson, “Review of artificial abrasion test methods for PV module technology,” Nat. Renewable Energy Lab., Lakewood, CO, USA, Tech. Rep.: NREL/TP-5J00-66334, 2016, doi: [10.2172/1295389](https://doi.org/10.2172/1295389).